Available online at www.sciencedirect.com
SCIENCE DIRECT®

Journal of the European Ceramic Society 23 (2003) 99–106

www.elsevier.com/locate/jeurceramsoc

Thermodynamic prediction of the nonstoichiometric phase $Zr_{1-z}Ce_zO_{2-x}$ in the ZrO_2–$CeO_{1.5}$–CeO_2 system

Shuigen Huang[a], Lin Li[a], Jef Vleugels[b], Peiling Wang[c], Omer Van der Biest[b,*]

[a]*School of Material Science and Engineering, Shanghai University, Shanghai 200072, China*
[b]*Department of Metallurgy and Materials Engineering, Katholieke Universiteit Leuven, B-3001 Heverlee, Belgium*
[c]*The State Key Lab of High Performance Ceramics and Superfine Microstructure, Shanghai Institute of Ceramics, Chinese Academy of Science, 200050 Shanghai, China*

Received 28 November 2001; accepted 3 March 2002

Abstract

A thermodynamic estimation of the ZrO_2–CeO_2 and ZrO_2–$CeO_{1.5}$ systems, as well as the cubic phase in the $CeO_{1.5}$–CeO_2 system has been developed and the complex relation between the nonstoichiometry, y, in Ce_zO_{2-y} and the oxygen partial pressure at different temperatures is evaluated. The behavior of the nonstoichiometry phase $Zr_{1-z}Ce_zO_{2-x}$ is described based on the thermodynamic estimation in the ZrO_2–CeO_2, $CeO_{1.5}$–CeO_2 and ZrO_2–$CeO_{1.5}$ systems. Additionally, the interdependence among miscellaneous factors, which can be used to describe the change in oxidation states of cerium such as the oxygen partial pressure, the $CeO_{1.5}$ fraction in $CeO_{1.5}$–CeO_2 in the quasi-ternary system, the nonstoichiometry y and the difference between the activity of CeO_2 and $CeO_{1.5}$ are predicted. The calculated results are found to be very useful to explain the influence of pressureless sintering at different O_2 partial pressures on the mechanical properties of CeO_2-stabilised ZrO_2 ceramics © 2002 Published by Elsevier Science Ltd.

Keywords: CeO_2; ZrO_2; Defects; Mechanical properties; Phase equilibria; Sintering

1. Introduction

Zirconia-based ceramics have attracted much attention in science and technology for many years, since ZrO_2 ceramics can be used for functional as well as structural applications. However, the volume change accompanying the martensitic phase transformation from the tetragonal (t) to the monoclinic (m) phase is large and destructive, which makes the material unsuitable to be used in the pure ZrO_2 state. Fortunately, it was revealed[1–4] that the addition of oxides, such as CeO_2, MgO, CaO or Y_2O_3, stabilizes the high temperature tetragonal or cubic phases.

It has been reported[4,6,7] that ceria-doped Ce-TZP (tetragonal zirconia polycrystal) exhibits an excellent thermal stability and extraordinary transformation plasticity and ferroelasticity. The excellent high toughness of zirconia ceramics is mainly caused by the stress-induced t→m martensite phase transformation.

Under ambient conditions, cerium forms two oxides, the stable dioxide, CeO_2, and the metastable sesquioxide, Ce_2O_3, incorporating Ce^{+4} and Ce^{+3} ions respectively. Under reducing atmospheric conditions and at elevated temperatures, CeO_2 can be reduced to a nonstoichiometnic CeO_{2-y} composition with $0.5 > y > 0$. When ceria-doped zirconia ceramics are exposed to an inert atmosphere or low oxygen partial pressure at elevated temperature, the Ce^{+4} will reduce to Ce^{+3} and the ZrO_2–CeO_2 system will convert to a quasi-ternary ZrO_2–CeO_2–$CeO_{1.5}$ system. Heussner et al.[8] introduced phase-transformation-induced compressive surface stresses into Ce-TZP through the reduction of CeO_2, and found that the four-point-bending strength of sintered 12 mol% CeO_2 stabilized ZrO_2 increased from 240 to 545 MPa after annealing at 1400 °C for 2 h in nitrogen. It is therefore important to carefully control the oxygen partial pressure in the ZrO_2–CeO_2–$CeO_{1.5}$ system, where the nonstoichiometric fluorite phase $Zr_{1-z}Ce_zO_{2-x}$ exists. It is also important to obtain the relation between the nonstoichiometry and oxygen partial pressure at different temperatures as it can be used as a guideline in the development of this type of ceramic materials.

* Corresponding author.
E-mail address: omer.vanderbiest@mtm.kuleuven.ac.be (O. Van der Biest).

0955-2219/02/$ - see front matter © 2002 Published by Elsevier Science Ltd.
PII: S0955-2219(02)00073-0

Lindemer et al.[9] studied the relation between the nonstoichiometry in the $U_{1-z}Ce_zO_{2-x}$ phase and the oxygen partial pressure, a system that is similar to the $Zr_{1-z}Ce_zO_{2-x}$ system investigated in this paper. They found that the UO_2–CeO_2 system changes to the UO_2–CeO_2–$CeO_{1.5}$ system in a low oxygen pressure environment at high temperature. Accordingly, the nonstoichiometry also changed with the change in oxygen pressure.

In the present work, the three limiting quasi-binary systems ZrO_2–CeO_2, ZrO_2–$CeO_{1.5}$ and $CeO_{1.5}$–CeO_2 are evaluated by the CALPHAD technique. In combination with the thermodynamic parameters of these systems, the relation between the stoichiometry, y, in the CeO_{2-y} phase and the oxygen partial pressure is calculated. The interdependence among miscellaneous factors, which can be used to describe the change in oxidation state of cerium in the $Zr_{1-z}Ce_zO_{2-x}$ system are discussed and tabulated. Sintering experiments under different O_2 partial pressures demonstrates the applicability of the calculated results for material development in the ZrO_2–$CeO_{1.5}$–CeO_2 system.

2. Assessment of the three quasi-binary systems

2.1. Experimental information on ZrO_2–CeO_2, ZrO_2–$CeO_{1.5}$ and $CeO_{1.5}$–CeO_2 systems

There are apparent discrepancies in the ZrO_2–CeO_2 system, especially in the high temperature ZrO_2-rich solid solution region as well as on the low temperature ordering phenomenon. In particular, significant discrepancies exist among the data of the phase equilibrium between t and m phases, as described in Refs. 4–6. Duran et al.[4] and Longo[5] found the existence of a quasi-binary $Zr_3Ce_2O_{10}$ compound through X-ray diffraction. This compound was stable below approximately 800 °C. They also suggested the existence of an eutectic reaction at 24 mol% CeO_2 at 2300 °C. However, Yashima et al.[6,7] reported they found no evidence of the metastable $Zr_3Ce_2O_{10}$ compound in their experiments. They also pointed out that the high temperature portion of the ZrO_2–CeO_2 system determined by earlier experiments was actually that of $(Zr^{+4},Ce^{+4},Ce^{+3})O^{-2}$, causing significant errors. In order to give a correct description of the system, Tani et al.[10] carefully adopted hydrothermal conditions to establish the real equilibrium to elucidate the phase diagrams of the ZrO_2–CeO_2 system. Based on experimental data of Tani et al.,[10] using the lattice stability parameters of liquid, cubic, tetragonal and monoclinic ZrO_2 phases from Du et al.,[3] Li et al.[11–13] optimized the system according to the sub-regular model.

Heussner et al.[8] pointed out that the ZrO_2–CeO_2 system will transform to the ZrO_2–$CeO_{1.5}$ system under certain experimental conditions. In the ZrO_2–$CeO_{1.5}$ system, the composition range of the cubic and tetragonal phase is totally different than in the ZrO_2–CeO_2 system. The Ce^{+4} cations will reduce to Ce^{+3} cations at increasing temperature in reducing atmosphere (H_2, CO, NH_3), under a vacuum of 10^{-1}–10^{-2} Pa (10^{-6}–10^{-7} bar), in inert atmospheres (Ar, He), as well as under a low oxygen partial pressure (1.4 Pa at 1400 °C). When the Ce^{+4} cations are partly reduced to the trivalent state, the ZrO_2–CeO_2 system transforms to the ZrO_2–CeO_2–$CeO_{1.5}$ system. According to previous reports[10–14] the ZrO_2–CeO_2 system has three single-phase regions, having the monoclinic (m), tetragonal (t) and cubic (c) symmetry, and a two-phase region where t + c is stable. In the ZrO_2–$CeO_{1.5}$ system, the cubic $Zr_2Ce_2O_7$ compound is stable, having a pyrochlore (p) structure and a composition range from 44 up to 57 mol% $CeO_{1.5}$. The p phase is in equilibrium with the monoclinic solid solution below 1000 °C and with the tetragonal phase above this temperature. There are three invariant reactions in the ZrO_2–$CeO_{1.5}$ system. Additional phase studies in the ZrO_2–Ce_2O_3 system have been conducted by Yoshimura et al.[14] at temperatures between 1350 °C and 1900 °C, confirming the existence of the p compound in the ZrO_2–$CeO_{1.5}$ system.

CeO_{2-y} is known to deviate strongly from its stoichiometric composition at elevated temperatures and reduced oxygen partial pressure to produce an oxygen deficient n-type semiconductor. In a series of X-ray and thermodynamic studies, it was demonstrated that reduced CeO_2 retains the cubic fluorite structure over an extended composition range at elevated temperatures. A miscibility gap region was shown by Ricken et al.[15] and Tuller et al.[16] to extend from CeO_2 to $CeO_{1.714}$ at temperatures above 722 K. Above 913 K, only one fluorite structure exists. Campserveux et al.[17] reported a diagram with a miscibility gap in the CeO_{2-y} system. At temperatures above 946 K, a single phase exists with $2 > 2-y > 1.818$. At temperatures below 722 K, CeO_{2-y} forms a discrete set of compositions extending from CeO_2 to $CeO_{1.8}$. Lindemer[9] also found that a single phase exists above 950 ± 20 K.

2.2. Thermodynamic model of three quasi-binary systems

A substitutional model is used to describe the quasi-binary systems, which estimates the mixing entropy of complex ceramic systems in a very simple way. Kaufman et al.,[18] Du et al.,[3,7] and Li et al.[11–13] already successfully evaluated oxide phase diagrams in this way.

In the present work, the experimental information on the ZrO_2–CeO_2 system is taken from Tani.[10] The system is re-optimized since the reference states in the present work and the former optimizations[3,11,12] are different. In the previous work,[3] liquid ZrO_2 was chosen as the reference state and lattice parameters of ZrO_2 in other

forms were deduced according to the thermodynamic information and experimental phase diagrams. In the present work, the Gibbs free energy of the cubic ZrO_2 structure is the standard free energy of formation from the elements in their stable states, taken from Ref. 19. Gibbs free energies of other phases of ZrO_2, CeO_2 and $CeO_{1.5}$ are retrieved from the corresponding quasi-binary phase diagrams.[10,17,20]

To calculate the diagram of the ZrO_2–$CeO_{1.5}$ system, the experimental data of Leonov et al.[20] are used and the p compound phase is simplified to be a stochiometric phase with 50 mol% $CeO_{1.5}$. This simplification will cause no error in the present estimation.

In order to obtain the $\ln(y)$–T–$\ln(Po_2)$ relation, the miscibility gap in the $CeO_{1.5}$ CeO_2 system is evaluated. The experimental data used are from Campserveux et al.[17] In this diagram, the highest temperature in the miscibility gap is 946 K, and only the $2>2-y>1.818$ data are taken into account to evaluate the thermodynamic coefficients. The other part of this system ($2-y<1.818$) is omitted because only the CeO_{2-y} phase is taken into account to describe the relation between $\ln(y)$ and $\ln(Po_2)$.

The Gibbs free energy of one mole solution phase, Φ is described as:

$$G_m^{\Phi}(x,T) = \sum_{i=1}^{2} x_i \cdot \Delta^{\circ} G_f^{\Phi-i}(T) + RT\sum x_i \ln x_i + x_1 x_2 \sum_{n=0}^{1} K^{n+3}(x_1 - x_2)^n \quad (1)$$

The first term on the right accounts for the mechanical mixture of the pure components. $\Delta^{\circ}G_f^{\Phi-i}(T)$ is the standard Gibbs free energy of formation of mass parameter i from the elements in their standard states. The second term refers to an ideal solution, and the third term is the excess Gibbs free energy function, which is a Redlich-Kister polynomial. The K^n factor in Eq. (1) is a temperature-related polynomial and is expressed as:

$$K^n = A^n + B^n T + C^n T\ln T + D^n T^2 + E^n/T + F^n T^3 \quad (2)$$

The Gibbs free energy of the stoichiometric compound phase with pyrochlore structure is described as:

$$G(1/4)Zr_2Ce_2O_7 = (1/2)\Delta^{\circ}G_f^{c-ZrO_2} + (1/2)\Delta^{\circ}G_f^{c-CeO_{1.5}} + A + B^*T \quad (3)$$

The thermodynamic calculations in the ZrO_2–$CeO_{1.5}$ system are conducted with a new version of the Lukas program (1996),[21] whereas the other systems are calculated using the Thermo-Calc (TC) program.

The calculated thermodynamic properties are listed in Tables 1 and 2. In Table 1, l-ZrO_2, c-ZrO_2, t-ZrO_2, m-ZrO_2 refer to the liquid, cubic, tetragonal and monoclinic phases of pure zirconia respectively. The same formalisms are used for the components of CeO_2 and $CeO_{1.5}$. In Table 2, Liq, Hss, Css, Tss, and Mss are used to represent the liquid, hexagonal, cubic, tetragonal, and monoclinic structures. The solution parameters of phases in the three quasi-binary systems and the Gibbs free energy of the stoichometric phase $Zr_2Ce_2O_7$ are also listed in Table 2.

The calculated phase diagram together with experimental literature data of the ZrO_2–CeO_2, ZrO_2–$CeO_{1.5}$ and $CeO_{1.5}$–CeO_2 systems are shown in Figs. 1–3 respectively. In Fig. 3, only the Css phase is considered, and is treated as a miscibility gap in the $CeO_{1.5}$–CeO_2 system.

3. Thermodynamic prediction of the nonstoichiometric phase $Zr_{1-z}Ce_zO_{2-x}$

3.1. Thermodynamic representation of the nonstoichiometric phase CeO_{2-y}

As suggested by Lindemer,[9] the representation used hereafter describes the chemical activities of cerium and oxygen in CeO_{2-y} using the thermodynamic properties of the two mass variables. One mass variable has the composition of the defect-free species, CeO_2, and the other, i.e. $CeO_{1.5}$, will be chosen to reflect together with CeO_2, the oxygen partial pressure–temperature–composition behavior and the system phase relations. In the $CeO_{1.5}$–CeO_2 system, it would be natural to list the formula:

$$4CeO_{1.5} + O_2 = 4CeO_2 \quad (4)$$

When the ZrO_2–CeO_2 system is exposed to an inert atmosphere or low oxygen pressure, it will convert to the ZrO_2–CeO_2–$CeO_{1.5}$ system. The $CeO_{2\sim}$phase exists in the CeO_2–$CeO_{1.5}$ system and the relation between the nonstoichiometry y and the oxygen partial pressure has already been investigated, suggesting that Zr–Ce–O data can be analyzed assuming that the system is composed of $(1-z)$ mole of ZrO_2 and z mole of CeO_{2-y}. The CeO_{2-y} is composed of m_2 mole CeO_2 and m_1 mole $CeO_{1.5}$. For nonstoichiometric phase $Zr_{1-z}Ce_zO_{2-x}$, the ratio O/(Ce + Zr) is obviously $2-x$. The O/Ce ratio in CeO_{2-y} can thus be calculated accordingly as:

$$2 - y = [2 - x - 2(1 - z)]/z \quad (5)$$

To obtain the $\ln(y)$–T–$\ln(Po_2)$ relation, one first needs to determine the number of moles, m_i, of each species. These are calculated from the mass-balance for cerium and oxygen as:

Table 1
Standard Gibbs free energy of formation (units in J/mol cation) of the ceramic components (298.15 K < T < 3200 K)

$\Delta^\circ G_f^{l-ZrO_2} = -1029045.10 + 239.90384^*T$
$\Delta^\circ G_f^{h-ZrO_2} = -1176169.65 + 179.52061^*T$
$\Delta^\circ G_f^{c-ZrO_2} = -1117031.17 + 269.3700^*T$
$\Delta^\circ G_f^{c-ZrO_2} = -1085836.00 + 100.221140^*T + 20^*T^*\mathrm{Ln}(T)$
$\Delta^\circ G_f^{m-ZrO_2} = -1118530.94 + 268.30049^*T$
$\Delta^\circ G_f^{l-CeO_2} = -900985.30 + 165.372^*T$
$\Delta^\circ G_f^{c-CeO_2} = -109555.0 + 235.39^*T$
$\Delta^\circ G_f^{t-CeO_2} = -1021682.17 + 210.55678^*T$
$\Delta^\circ G_f^{m-CeO_2} = 4321866.00 - 2481.86958^*T$
$\Delta^\circ G_f^{l-CeO_{1.5}} = -881375.72 + 130.62885^*T$
$\Delta^\circ G_f^{h-CeO_{1.5}} = -890588.90 + 164.37484^*T$
$\Delta^\circ G_f^{c-CeO_{1.5}} = -890588.90 + 164.37484^*T$
$\Delta^\circ G_f^{t-CeO_{1.5}} = 5520853.97 + 520.7109^*T$

Table 2
Optimized interaction parameters

Phase	Reference state		K^3 [J/(mol of cation)]	K^4 [J/(mol of cation)]	K^5 [J/(mot of cation)]
ZrO_2–$CeO_{1.5}$ system					
Liq	Liq	Liq	$56270.42–26.08355^*T$	$228954.09–73.21097^*T$	$-225766.65+79.60327^*T$
Css	c-ZrO_2	c-$CeO_{1,5}$	$318780.81–1\ 68.98530^*T$	$407393.98–173.72671\ ^*T$	
Hss	h-ZrO_2	h-$CeO_{1.5}$	$928326.32.62.86435^*T$	$-82160663+14570470^*T$	
Tss	t-ZrO_2	t-$CeO_{1.5}$	-7504461.21		
ZrO_2–CeO_2 system					
Liq	Liq	Liq	$-245224.18+58.35807^*T$	$-129113.78+49.50130^*T$	
Css	c-ZrO_2	c-CeO_2	$108233.71–56.62258^*T$	$-6395050+2654790^*T$	
Tss	t-ZrO_2	t-CeO_2	$-29329.38+2.83256^*T$		
Mss	m-ZrO_2	m-CeO_2	$-5656207.45+2886.86323\ ^*T$		
$CeO_{1.5}$–CeO_2 system					
Css	c-$CeO_{1.5}$	c-CeO_2	$-70210+32.05^*T$	$-63965+32.05^*T$	
$Zr_2Ce_2O_7$ compound					
$G(1/4)Zr_2Ce_2O_7 = (1/2)\Delta^o G_f^{c-ZrO_2} + (1/2)\Delta^o G_f^{c-CeO_{1.5}} + 50613.29-39.20788^*T$(J/mol of cation)					

$$z = m_2 + m_1 \quad \text{and} \quad z(2-y) = 2m_2 + 1.5m_1 \tag{6}$$

which leads to

$$m_1 = 2zy, \quad m_2 = z(1-2y) \tag{7}$$

In a system without ZrO_2 component [z = 1 (mole)], the mole fraction of $CeO_{1.5}$ is $N_1 = m_1/(m_1+m_2)$ and the mole fraction of CeO_2 is $N_2 = m_2/(m_1+m_2)$. Moreover, $y = 0.5–0.5N_2$.

Based on the thermodynamic information of the limiting quasi-binary systems, the molar Gibbs free energy of the nonstoichiometric phase $Zr_{1-z}Ce_zO_{2-x}$ can be written according to Maggianu[22] as:

$$\begin{aligned} G' &< Zr_{1-z}Ce_zO_{2-x} > /(m_1+m_2+m_3) \\ &= N_1\Delta^\circ G_f^{Css-CeO_{1.5}} + N_2\Delta^\circ G_f^{Css-CeO_2} \\ &+ N_3\Delta^\circ G_f^{Css-ZrO_2} + N_1RT\ln(N_1) + N_2RT\ln(N_2) \\ &+ N_3RT\ln(N_3) + K_{1,2}^3N_1N_2 + K_{1,2}^4N_1N_2(N_1-N_2) \\ &+ K_{1,3}^3N_1N_3 + K_{1,3}^4N_1N_3(N_1-N_3) + K_{2,3}^3N_2N_3 \\ &+ K_{2,3}^4N_2N_3(N_2-N_3) \end{aligned} \tag{8}$$

where $\Delta^\circ G_f^{Css-i}$ is the standard Gibbs free energy of formation of mass parameter i from the elements in their standard states. $\Delta^\circ G_f^{Css-ZrO_2}$ is after the compilation of Pankratz,[19] whereas and $\Delta^\circ G_f^{Css-CeO_{1.5}}$ are retrieved from the quasi-binary phase diagrams as shown in Table 1. $K_{i,j}^n$ is the interaction coefficient as shown in Table 2, where n is the order of the Redlich–Kister polynomial and the subscripts i,j represent the components, i.e., $CeO_{1.5}=1$, $CeO_2=2$, $ZrO_2=3$. N_i (i=1,2,3) is the molar fraction of $CeO_{1.5}$, CeO_2 and ZrO_2 respectively.

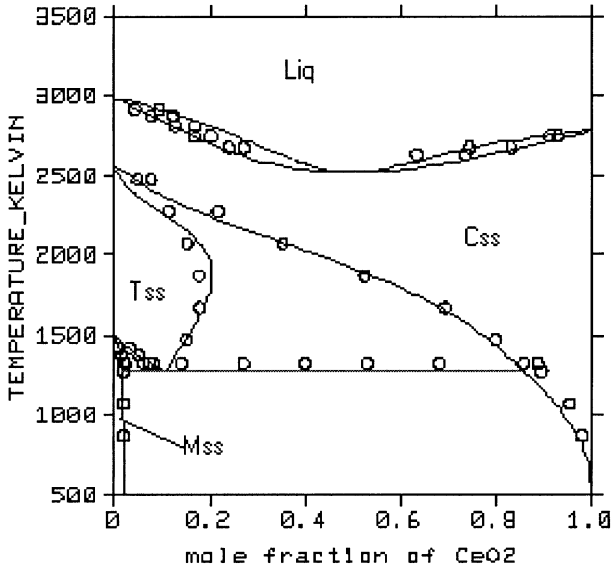

Fig. 1. Calculated phase diagram of the ZrO_2–CeO_2 system, open circles referring to the experimental results taken from Ref. 10.

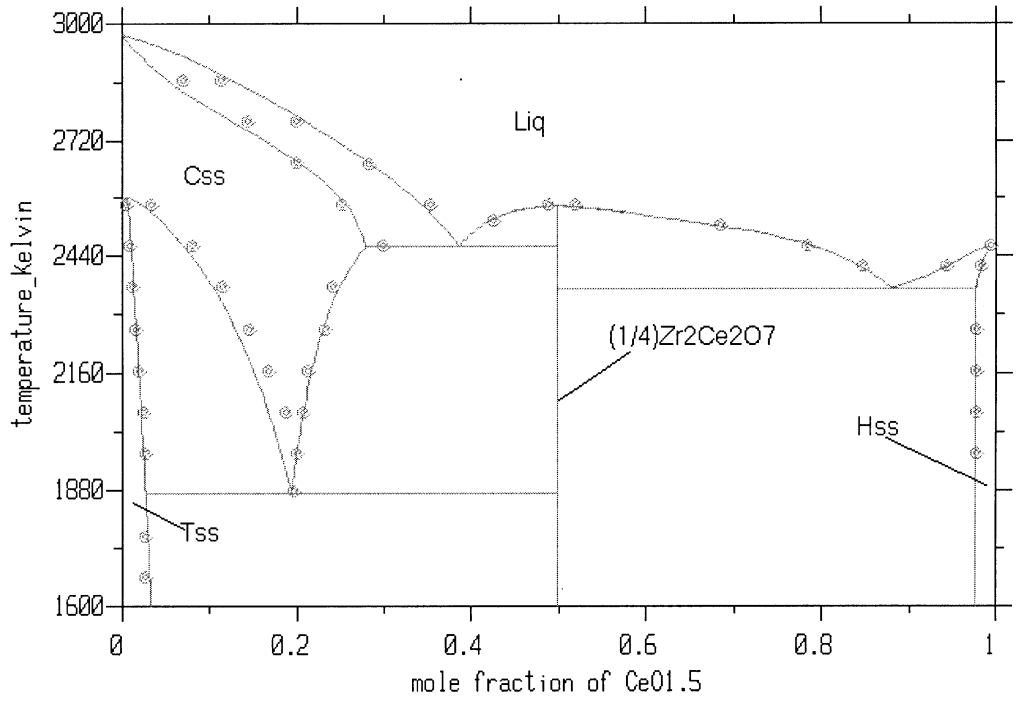

Fig. 2. Calculated phase diagram of the ZrO_2–$CeO_{1.5}$ system, symbols referring to the experimental results taken from Ref. 20.

The general equation for the partial molar Gibbs free energy of each mass parameter is needed in order to calculate the free energy change for Eq. (4).

The partial molar free energy for mass parameter i equals to,

$$\partial[G'Zr_{1-z}Ce_zO_{2-x}]/\partial m_i = \Delta\overline{G}_i \tag{9}$$

Eqs. (4), (8) and (9) lead to an equation to evaluate the ln(y)–ln(Po_2) relation in the ZrO_2–$CeO_{1.5}$–CeO_2 system. Since the free energy difference for Eq. (4) is $4\Delta\overline{G}_{CeO_2} - 4\Delta\overline{G}_{CeO_{1.5}}$, the oxygen partial pressure is given by:

$$RT\ln(Po_2) = 4\Delta\overline{G}_{CeO_2} - 4\Delta\overline{G}_{CeO_{1.5}} \tag{10}$$

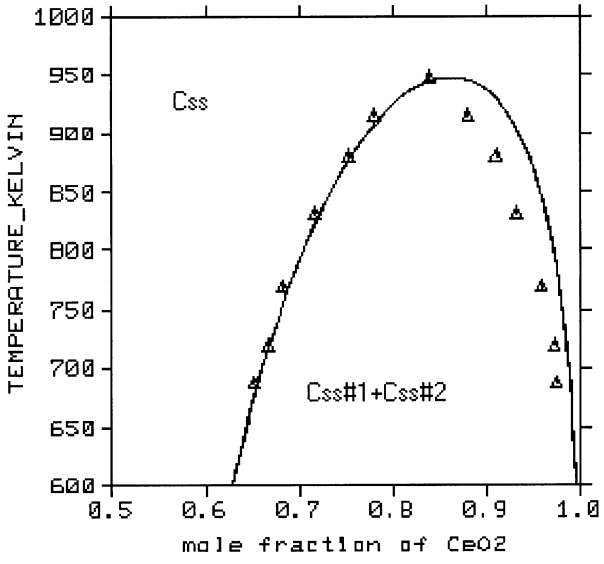

Fig. 3. Calculated and experimental Css phase region in the $CeO_{1.5}$–CeO_2 system, triangles representing the experimental data reported in Ref. 17.

$CeO_{1.5}$ and CeO_2 are the only components when $z=1$, $m_3=0$ and $N_3=0$. In that case, the relation between ln(y) and ln(Po_2) can be obtained from Eq. (10). The relevant portion of the calculated curves consist of the y, T and Po_2 interdependence. The temperature, T is in Kelvin, y is the deviation from stoichiometry and Po_2 is the pressure of oxygen in unit of MPa divided by the standard state oxygen pressure, 0.101 MPa.

The calculated results at 1773 K, 1573 K, 1473 K are shown in Fig. 4 and are found to be in excellent agreement with the plotted experimental data, taken from Ref. 9.

3.2. Thermodynamic prediction of the nonstoichiometric phase: $Zr_{1-z}Ce_zO_{2-x}$

At present, there is very little experimental information on $Zr_{1-z}Ce_zO_{2-x}$, and no reports at all about the relation between ln(y) and ln(Po_2). To study the ZrO_2–CeO_2 system for practical purposes, the inert atmosphere and especially the oxygen partial pressure must be taken into consideration. When $z<1$ (mole), part of the CeO_2 has transformed to $CeO_{1.5}$. According to Eqs. (8)–(10), the transformed part can be evaluated when the $\Delta^\circ G_f^{Css-i}$ parameters and $K_{i,j}$ interaction coefficients are known.

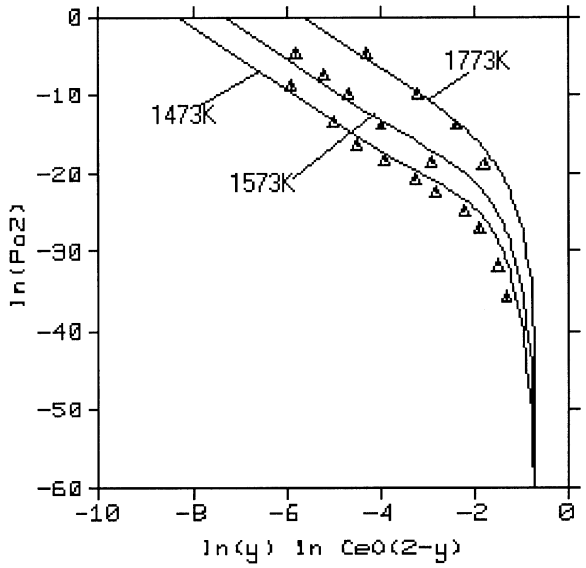

Fig. 4. Calculated relationship between ln(y) and ln(PO_2), triangles representing the experimental results reported in Ref. 9.

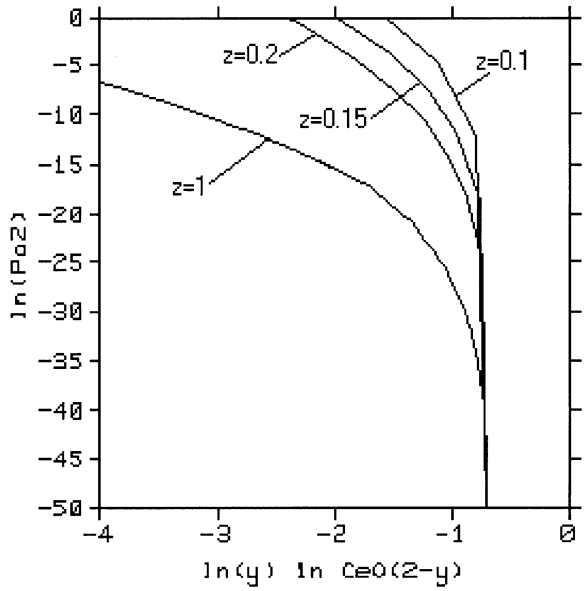

Fig. 6. Predicted relationship between ln(y) and ln(PO_2) at 1773 K at different $CeO_{2-y;}$ molar fractions in the ZrO_2–$CeO_2CeO_{1.5}$ system.

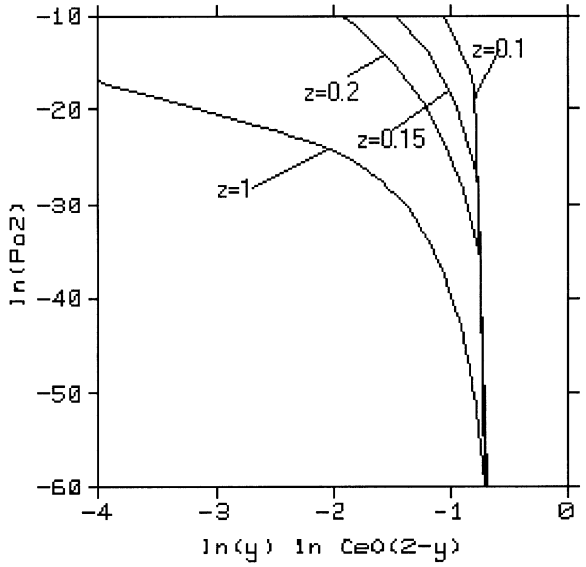

Fig. 5. Predicted relationship between ln(y) and ln(PO_2) at 1473 K at different CeO_{2-y} molar fractions in the ZrO_2–CeO_2–$CeO_{1.5}$ system.

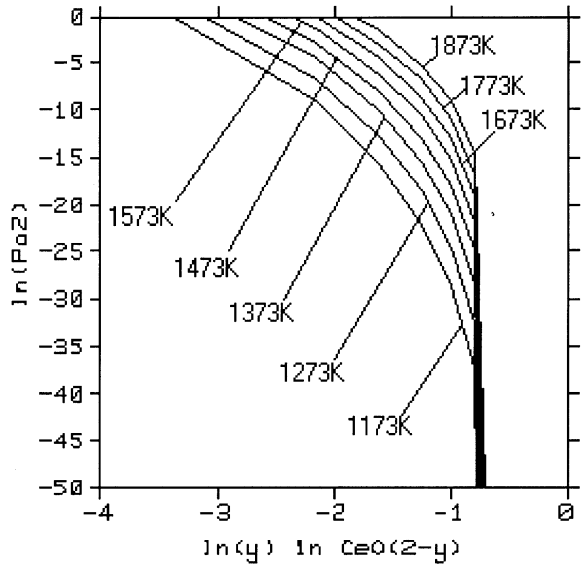

Fig. 7. Predicted relationship between ln(y) and ln(PO_2) as function of temperature at a fixed ZrO_2 molar fraction 0.85 ($z = 0.15$) in the ZrO_2–CeO_2–$CeO_{1.5}$ system.

In the present work, the three quasi-binary systems have been evaluated, and the parameters needed are all listed in Tables 1 and 2, allowing to approach the complex relations. The calculated results are graphically presented in Figs. 5–7.

In Fig. 5, the different lines represent different molar fractions of CeO_{2-y} ($z = 0.1$, 0.15, 0.2 and 1.0) corresponding to different ZrO_2 molar fractions (0.9, 0.85, 0.8, 0) in the ternary Zr–Ce–O system at 1473 K. The influence of the ZrO_2 content in the material, represented by the z value, on the relation between the oxygen partial pressure and the stoichiometry value is significant.

Similar estimations are made at 1773 K, as presented in Fig. 6. Fig. 7 reveals that at a ZrO_2 content of 85 mol%, the CeO_{2-y} stoichiometry is strongly influenced by the oxygen pressure and temperature.

4. Experiments with CeO_2-stabilized ZrO_2

Commercially available 12 mol% CeO_2-stabilized co-precipitated ZrO_2 powder, Daiichi grade CEZ12, was cold isostatically pressed (CIPed) into cylinders, with a diameter of 1 cm and a length of 2 cm, under a pressure

Table 3
Calculated DGF, y and molar fraction of $CeO_{1.5}$ and mechanical properties of Ce-TZP ceramics sintered at 1723 K in different atmospheres

Atmosphere	Detected PO_2 (Pa)	Calculated PO_2 (Pa)	DGF (J/mole cation)	y in CeO_{2-y}	$CeO_{1.5}/(CeO_{1.5}+CeO_2)$	Density (g/cm^3)	H_v (kg/mm^2)	K_{IC} (MPa $m^{1/2}$)
Synthetic air	2.03 E+04	2.04E+04	−4.00E-01	1.38E-01	2.76E-01	6.20	1059±12	6.6 ±0.3
Air + Ar(50/50)	1.01 E+04	1.01E+04	−5.76E-01	1.51E-01	3.01E-01	6.20	1021 ±25	6.3±1.0
Ar + air(90/10)	2.03 E+03	2.07E+03	−9.72E-01	1.81E-01	3.62E-01	6.20	1019±12	6.4±0.3
N_2	0.30	1.91E-01	−3.30E+00	3.64E-01	7.29E-01	6.12	927±53	12.7±2.0
Ar + N_2(90/10)	0.12	1.14E-0l	−3.42E+00	3.73E-01	7.46E-01	6.18	915±10	13.4±1.0
Ar	0.10	1.14E-01	−3.42E+00	3.73E-01	7.46E-01	6.16	902±22	16.2±0.5
Vacuum in graphite furnace	$<2.00\times10^{-3}$	2.64E-04	−4.94E+00	4.52E-01	9.05E-O1	Cracked	–	–

of 300 MPa for 3 min. The powder compacts are sintered at 1450 °C (1723 K) in the alumina tube furnace of a TGA (Cahn TG-l71) with a heating rate of 20 °C/mm and a cooling rate of 50 °C/min down to 1000 °C, followed by natural cooling. Sintering is performed under a gas flow of 75 ml/min. The gasses used are synthetic air (L'Air Liquide N20, 20% 02, 10 ppm H_2O), nitrogen (L'Air Liquide N28, 3 ppm O2) and argon (L'Air Liquide N50, 5 ppm N_2, 1 ppm O2). Air–argon and argon–nitrogen mixtures are obtained using a gas flow meter (model 5878, Brooks Instruments B.V.). An additional sample is sintered in vacuum ($<2\times 10^3$ Pa) in a graphite furnace.

The hardness and fracture toughness of the sintered samples are determined by the Vickers indentation method with an indentation load of 10 and 30 kg on polished cross-sectioned samples. The fracture toughness is calculated according to the formula of Anstis et al.[23] The E-modulus of the air-sintered ceramic, 210 MPa, as measured by the impulse excitation technique,[24] is used in all toughness calculations. The density is determined in ethanol.

The influence of sintering in different atmospheres on the mechanical properties is summarized in Table 3. The density, hardness and fracture toughness of the Ce-TZP ceramics is the same at oxygen partial pressures above 2000 Pa. Decreasing the PO_2 of the sinter atmosphere down below 0.3 Pa decreases the hardness with about 100 kg/mm^2, whereas the fracture toughness is spectacularly increased from 6.5 up to a maximum of 16.2 MPa $m^{1/2}$. The fracture toughness is found to strongly increase with decreasing PO_2 levels in the region between 0.3 and 0.1 Pa.

The DGF (the difference between the activities of CeO_2 and $CeO_{1.5}$, i.e., $a_{CeO_2} - a_{CeO_{1.5}}$), the non-stoichiometry y of CeO_{2-y} and the molar fraction ratio of $CeO_{1.5}$ in ($CeO_{1.5}+CeO_2$) are calculated as a function of oxygen partial pressure (in Pa) at 1723 K. During calculation, the mole fraction of ZrO_2 is assumed to be 0.8344, which is close to the value in the tested samples.

The experimental results can be interpreted by the estimated results shown in Table 3. Estimation reveals that at 1450 °C (1723 K) under a oxygen partial pressure of 2.04×10^4 Pa, which is almost the same as that of oxygen in the global atmosphere,[25] the equilibrium content of $CeO_{1.5}$ in ($CeO_{1.5}+CeO_2$) is about 27.6%. Visual inspection of the cross-sectioned samples sintered in air indeed revealed a color change from white to green towards the center of the sintered cylinders, which is a clear indication of the reduction phenomena that occurred during sintering. Sintering of the powder compacts at PO_2 levels between 0.1 and 0.3 Pa resulted in homogeneously dark colored fully dense samples with significantly increased fracture toughness as well as a small decrease in hardness. The thermodynamic calculations reveal that the relevant portion of $CeO_{1.5}$ in ($CeO_{1.5}+CeO_2$) reaches 72.9% at a PO_2 level of 0.191 Pa. At calculated $CeO_{1.5}$ molar fractions above 0.9, the samples were found to spontaneously transform, resulting in completely cracked samples.

5. Conclusion

The complex thermodynamic interdependence of temperature, nonstoichiometry and oxygen partial pressure in $Zr_{1-z}Ce_zO_{2-x}$ was presented. For the first time, this complex relation is predicted, based on the thermodynamic study of the equilibrium between O_2, CeO_{15} and CeO_2. Since the nonstoichiometry and the temperatures are calculated in the region of engineering interest, it is believed that the calculated results are very instructive to the sintering practice and engineering of CeO_2-stabilised zirconia-based ceramics.

Acknowledgements

This work is financially supported by the Flanders-China bilateral project (BIL 99/10), the Science and Technology Committee of the Shanghai Municipality, the State Key Lab of High Performance Ceramics and Superfine Microstructure of Chinese Academy of Science and the Commission of the European Communities in

the framework of the Growth project "BIOGRAD" (G5RD-CT2000-00354). The authors are thankful to Prof. H.L. Lukas for offering the new version of the Lukas Program.

References

1. Hannink, R. H. J., Kelly, P. M. and Muddle, B. C., Transformation toughening in zirconia-containing ceramics. *J. Am. Ceram. Soc*., 2000, **83**, 461–487.
2. Rouanet, A., High temperature solidification and phase diagrams of the ZrO2-Er_2O_3, ZrO_2-Y_2O_3 and ZrO_2-Yb_2O_3 systems. *C. R. Seances Acad. Sci., Ser. C*, 1968, **267**, 1581–1584.
3. Du, Y., Jin, Z. P. and Huang, P. Y., Thermodynamic assessment of the ZrO_2-$YO_{1.5}$ system. *J. Am. Ceram. Soc*., 1991, **74**, 1569–1577.
4. Duran, P., Gonzalez, M., Moure, C., Jurado, J. R. and Pascual, C., A new tentative phase equilibrium diagram for the ZrO_2-CeO_2 system in air. *J. Mater Sci*., 1990, **25**, 5001–5006.
5. Longo, V. and Minichelli, D., X-ray characterization of $Ce_2Zr_3O_{10}$. *J. Am. Ceram. Soc*., 1973, **56**, 600.
6. Yashima, M., Takshina, H., Kakihana, M. and Yoshimura, M., Low-temperature phase equilibria by the flux method and the metastable-stable phase diagram in the ZrO_2-CeO_2 system. *J. Am. Ceram. Soc*., 1994, **77**, 1869–1874.
7. Du, Y., Yashima, M., Koura, T., Kakihana, M. and Yoshimura, M., Thermodynamic evaluation of the ZrO_2-CeO_2 system. *Scripta Metall. Mater*., 1994, **31**, 327–332.
8. Heussner, K.-H. and Claussen, N., Strengthening of ceria-doped tetragonal zirconia polycrystals by reduction-induced phase transformation. *J. Am. Ceram. Soc*., 1989, **72**, 1044–1046.
9. Lindemer, T. B. and Brynestad, J., Review and chemical thermodynamic representation of $<U_{1-z}Ce_zO_{2\pm x}>$ and $<U_{1-z}Ln_zO_{2\pm x}>$; Ln = Y, La, Nd, Gd. *J. Am. Ceram. Soc*., 1986, **69**, 867–876.
10. Tani, E., Yoshimura, M. and Somiya, S., Revised phase diagram of the system ZrO_2-CeO_2 below 1400 °C. *J. Am. Ceram. Soc*., 1983, **66**, 506–510.
11. Li, L., Xu, Z. Y. and Ao, Q., Optimization of the phase diagram of CeO_2-ZrO_2 system. *J. Mater Sci. Tech*., 1996, **12**, 159–160.
12. Li, L., Van Der Biest, O., Wang, P. L., Vleugels, J., Chen, W. W. and Huang, S. G., Estimation of the phase diagram in the ZrO_2-Y_2O_3-CeO_2 system. *J. Eur. Ceram. Soc*., 2001, **21**(16), 2903–2910.
13. Li, L., Van Der Biest, O., Xu, L. P., Vleugels, J. and Huang, S. G., Prediction of the isothermal sections of the ZrO_2-Y_2O_3-CeO_2 system. *J. Mater. Sci. Tech*., 2001, **17**(5), 529–534.
14. Yoshimura, M. and Sata, T., Phase studies on the system ZrO_2-Ce_2O_3 from 1350 °C to 1900 °C. *Bull. Tokyo Inst. Technol*., 1972, **108**, 25–32.
15. Ricken, M., Noelting, J. and Riess, I., Specific heat of non-stoichiometric ceria (*CeOy*). *Solid State Ionics*, 1986, **18/19**, 725–726.
16. Tuller, H. L. and Nowick, A. S., Defect structure and electrical properties of nonstoichiometric CeO_2 single crystals. *J. Electrochem. Soc*., 1976, **126**, 209–217.
17. Campserveux, J. and Gerdanian, P., Etude thermodynamique de I'oxyde CeO_{2-x} pour $1.5 < O/Ce < 2$. *J. Solid State Chem*., 1978, **23**, 73–92.
18. Kaufman, L. and Nesor, H., Calculation of quasi-binary and quasi-ternary oxide systems I. *CALPHAD*, 1978, **2**, 35–53.
19. Pankratz, L. B., *Thermodynamic Properties of the Elements and Oxides*. US Dept. Interior, Bureau of Mines Bulletin 672, US Gov't Printing office, Washington, DC, 1982.
20. Leonov, A. I., Keler, E. K. and Andreeva, A. B., *Izv. Akad. Nauk SSSR. Inorg. Mater*., 1996, **2**, 1047–1049.
21. Lukas, H. L., Hening, E.Th. and Zimmermaim, B., Optimization of phase diagrams by a least squares method using simultaneously different types of data. *CALPHAD*, 1977, **1**, 225–236.
22. Muggianu, Y. M., Gambino, M. and Bros, J. P., Enthalpies de formation des alliages liquides bismuth-etain-gallium a 723 K. *J. Chim. Phys*., 1975, **22**, 83–88.
23. Anstis, G. R., Chantikul, P., Lawn, B. R. and Marshall, D. B., A critical evaluation of indentation techniques for measuring fracture toughness: I, direct crack measurements. *J. Am. Ceram. Soc*., 1981, **64**, 533–538.
24. Roeben, G., Bollen, B., Brebels, A., Van Humbeeck, J. and Van Der Biest, O., Impulse excitation apparatus to measure resonant frequencies, elastic moduli, and internal friction at room and high temperature. *Rev. Sci. Instr*., 1997, **68**, 4511–4515.
25. Lide, D. R., *Handbook of Chemistry and Physics*, 79th ed. CRC Press, New York, 1998/1999.